PARAMETRIC AMPLIFIER INPUT NOISE TEMPERATURE DEGRADATION CAUSED BY AN INTERFERING SIGNAL IN OR NEAR THE PARAMP PASSBAND

William Standish Phillips

Naval Postgraduate School
Monterey, California

June 1972

NAVAL POSTGRADUATE SCHOOL
Monterey, California

THESIS

PARAMETRIC AMPLIFIER INPUT NOISE TEMPERATURE DEGRADATION CAUSED BY AN INTERFERING SIGNAL IN OR NEAR THE PARAMP PASSBAND

by

William Standish Phillips

Thesis Advisor: G. L. Sackman

June 1972

Approved for public release; distribution unlimited.

50

Security Classification

DOCUMENT CONTROL DATA - R & D

(Security classification of title, body of abstract and indexing annotation must be entered when the overall report is classified)

1 ORIGINATING ACTIVITY (Corporate author)	2a. REPORT SECURITY CLASSIFICATION
Naval Postgraduate School Monterey, California 93940	Unclassified
	2b. GROUP

3 REPORT TITLE

Parametric Amplifier Input Noise Temperature Degradation Caused by an Interfering Signal in or Near the Paramp Passband

4 DESCRIPTIVE NOTES (Type of report and inclusive dates)

Master's Thesis; June 1972

5 AUTHOR(S) (First name, middle initial, last name)

William Standish Phillips

6 REPORT DATE	7a. TOTAL NO. OF PAGES	7b. NO. OF REFS
June 1972	50	12

8a. CONTRACT OR GRANT NO.	9a. ORIGINATOR'S REPORT NUMBER(S)
b. PROJECT NO	
c.	9b. OTHER REPORT NO(S) (Any other numbers that may be assigned this report)
d.	

10 DISTRIBUTION STATEMENT

Approved for public release; distribution unlimited.

11. SUPPLEMENTARY NOTES	12. SPONSORING MILITARY ACTIVITY
	Naval Postgraduate School Monterey, California 93940

13 ABSTRACT

The dependence of the input noise temperature of a parametric amplifier upon the pump source AM noise level, when a strong interfering signal is present in or near the paramp passband, is examined both theoretically and experimentally. An equation has been derived that predicts a contribution to the paramp input noise temperature which is linearly proportional to interfering signal power, paramp gain, and pump AM noise level. Experimental verification was achieved in comparison of various klystron, gunn, and impatt oscillator pumps exciting a typical military satellite communication receiver paramp.

DD FORM 1 NOV 68 1473 (PAGE 1)

S/N 0101-807-6811

Security Classification

A-31

14 KEY WORDS	LINK A		LINK B		LINK C	
	ROLE	WT	ROLE	WT	ROLE	WT
Low Noise Amplifier						
Amplifier						
Parametric Amplifier						
42 GHz						
Silicon Impatt Pump						
Low Noise						
Interfering Signal						
Pump Noise						
Satellite Communication Receiver						
Military Communications Receiver						
X-Band Amplifier						

DD FORM 1 NOV 65 1473 (BACK)

S/N 0101-807-6811

Parametric Amplifier Input Noise Temperature Degradation Caused by an Interfering Signal in or Near the Paramp Passband

by

William Standish Phillips
Lieutenant, United States Navy
B.S.E.E., Purdue University, 1965

Submitted in partial fulfillment of the requirements for the degree of

MASTER OF SCIENCE IN ELECTRICAL ENGINEERING

from the

NAVAL POSTGRADUATE SCHOOL
June 1972

Author William S Phillips

Approved by: Geo L Luckman
Thesis Advisor

Sydney R Parker
Chairman, Department of Electrical Engineering

Milton J Harrell
Academic Dean

ABSTRACT

The dependence of the input noise temperature of a parametric amplifier upon the pump source AM noise level, when a strong interfering signal is present in or near the paramp passband, is examined both theoretically and experimentally. An equation has been derived that predicts a contribution to the paramp input noise temperature which is linearly proportional to interfering signal power, paramp gain, and pump AM noise level. Experimental verification was achieved in comparison of various klystron, gunn, and impatt oscillator pumps exciting a typical military satellite communication receiver paramp.

TABLE OF CONTENTS

LIST OF TABLES

LIST OF FIGURES

ACKNOWLEDGEMENT

I wish to thank the Commander, Naval Electronics Laboratory Center San Diego, California, for the use of the laboratory facilities at the center. I especially wish to thank Ken D. Regan; (Communications Systems Branch, Microwave Technology Divison Code 2300, for the Satellite Program Office Code 1400) at the center, for his guidance, assistance, and loan of equipment, which made this project possible.

I. INTRODUCTION

While the principle of parameteric amplification has been known for some time, only in the past ten years have they found wide usage in military applications. The development of a high frequency cutoff varactor diode has made the low noise temperature paramp a practical device.

The technical journals abound with papers on paramp design, however, the effect on amplifier noise temperature of AM noise in the pump source has been virtually ignored by current authors. This was partly justified since klystron AM noise levels are low enough to make these contributions negligible.

With the advance of solid state technology, high power fundamental frequency generation devices are now replacing klystrons as paramp pump sources. Some of these solid state devices have a high AM noise level and in some applications may degrade a paramp's operating performance.

This work complements the continuing work being done by K. D. Regan (Communication Systems Branch, Microwave Technology Division code 2300, for the Satellite Program Office code 1400, Naval Electronics Laboratory, San Diego, California). References 1 through 4 contain investigacive information about military parametric amplifiers.

A. SATCOM EARTH RECEIVE TERMINAL G_r/T AS A SYSTEM FIGURE OF MERIT

A measure of goodness for a satcom earth receive terminal is directly related to G_r/T, where G_r is the antenna gain and

T is the input system noise temperature. The specification of G_r/T for a particular satellite receiver will guarantee a minimum signal power to noise power ratio at the input of the parametric amplifier.

For a specified data rate that a communication channel must support:

$$R = \frac{C/N_t}{E_b/N_o} \qquad (1)$$

where; R = desired data rate

E_b/N_o = ratio of energy per bit to noise power density required to decode at an acceptable error rate; this ratio depends upont the type of modulation used

C/N_t = ratio of the received carrier power to the total noise power density measured at the receiving terminal

The total useful satellite power C referenced at the input of the parametric amplifier is:

$$C = \frac{kP_sG_r}{L_d} \qquad (2)$$

where: G_r = receiving antenna gain

L_d = downlink propagation loss

P_s = satellite effective radiated power (ERP)

k = fraction of the satellite ERP alloted to the communication channel ($0 \leq k \leq 1$)

The total noise power density as seen at the input of the parametric amplifier is:

$$N_t = N_r + N_s \qquad (3)$$

$$N_r = KT \quad \text{per Hz bandwidth} \qquad (4)$$

$$N_s = \frac{(1-k)P_s}{L_d W} \tag{5}$$

where: K = BOLTZMAN'S constant

T = input noise temperature

W = operating bandwidth of the satellite

Combining equations 2, 4, and 5:

$$C/N_t = \frac{\frac{kP_sG_r}{L_dKT}}{1 + \frac{(1-k)P_sG_r}{L_dKWT}} \tag{6}$$

For a typical satellite terminal:

$$1 >> \frac{(1-k)P_sG_r}{L_dKWT} \tag{7}$$

therefore:

$$C/N_t = \frac{k\ P_s}{L_dK} \cdot \frac{G_r}{T} \tag{8}$$

Since G_r/T is a receiver function only it may be referred to as the receiver system figure of merit.

G_r is a function of the physical dimension of a typical parabolic antenna. From Equation 8 the receiver system input noise temperature T should be made as small as possible and is the reason for the great amount of effort that is being put into the development of highly reliable low noise amplifiers.

B. RECEIVER SYSTEM NOISE TEMPERATURE T

The earth receive terminal noise temperature (T) is determined by a number of basic subsystems. These subsystems include:

a. The low noise antenna providing high gain with small contributions to the overall noise temperature.
b. The feed system losses in the antenna structure.
c. The low noise receiver temperature contribution.
d. Additional amplification stages following the paramp.

Summing the individual noise temperature contributions:

$$T = T_{antenna} + T_{losses} + T_{paramp} + \frac{T_{additional\ stages}}{Gain\ Paramp} \qquad (9)$$

The noise temperature contributions for a parabolic antenna include; cross polarization loss, forward spillover loss, scattering and blockage loss. The sky also has a contributing noise temperature which varies from about 3.5 kelvins at the zenith to 240 kelvins on the ground. The antenna will sum the various noise contributions and a plot of antenna noise temperature versus elevation angle can be made as in Figure 1.

The antenna noise temperature will never be significantly below 10 kelvins and typical values will range in the 30-60 kelvins range as reported by Cuccia [Ref. 5].

The feed and other plumbing loss noise temperature contributions will be approximately 15 kelvins also reported by Cuccia [Ref. 5].

$$T_{losses} = (L - 1)T_o \qquad (10$$

where: T_o = 290 Kelvins
L = loss factor

From Equation 10 for a loss of .1 DB a noise temperature of 7.2 Kelvins will result. Because of this, plumbing losses must be kept to a minimum.

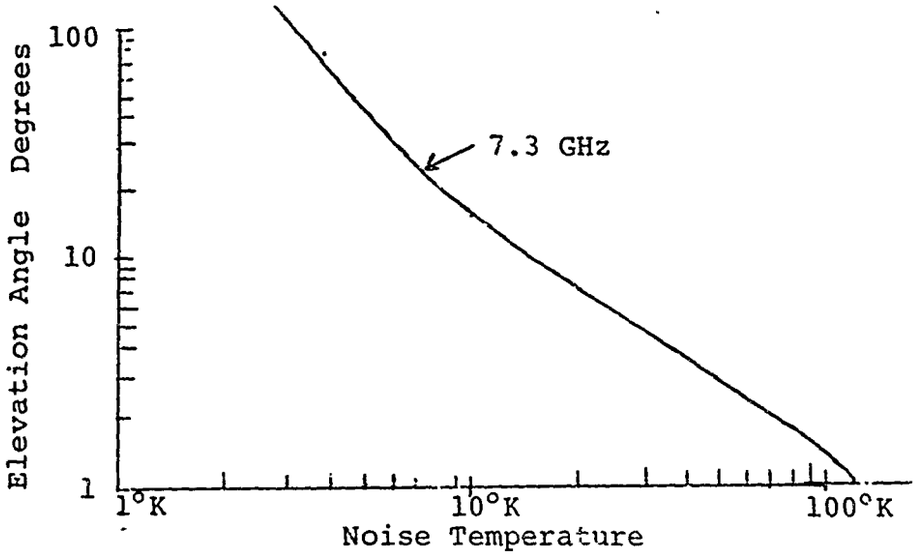

Figure 1. Antenna Elevation Angle Versus Temperature

Figure 2 compares the noise temperature of several different types of low noise receivers that may be considered depending upon the system requirements.

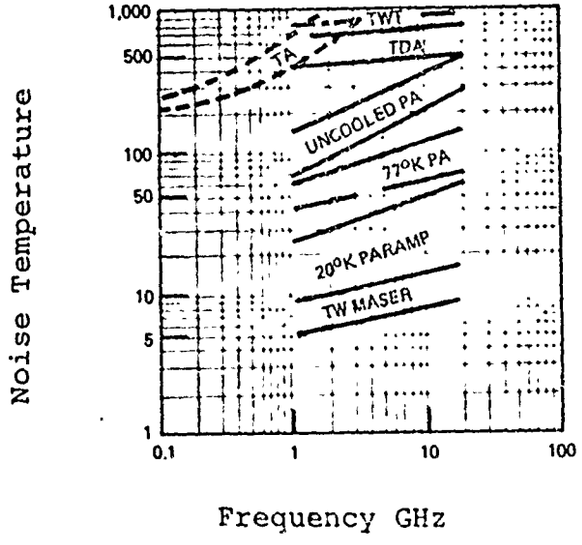

Figure 2. Input Noise Temperature Versus Frequency for Various Types of Low Noise Receivers

Considering the various types of receivers and the noise temperature requirements, system designers are utilizing the uncooled paramp for a wide range of low noise temperature applications. For systems that do not require a very low noise temperature input, the tunnel diode amplifier is widely used. The tunnel diode is less costly, has a higher reliability factor, and is easier to maintain than a paramp. If the input noise temperature of the tunnel diode can be reduced through additional advances in solid state technology, the TDA may replace the paramp in many low noise temperature amplifier applications.

II. THE PARAMETRIC AMPLIFIER

The theory of operation of a single stage reflex nondegenerate parametric amplifier is well understood. Heffner and Wade, [Ref. 6], published a paper that formalized the gain, bandwidth, and noise characteristics of a parametric amplifier, Penfield and Rafuse, [Ref. 7], published a book on Varactor Applications that is still considered to be designer's bible for the design of parametric amplifiers. Nearly all other authors in their works address one or more of the problems as listed in Table I.

TABLE I. PARAMP CONSIDERATIONS

Noise Temperature	Reliability	Maintainability
Gain	Input Impedance	Pump Leakage
Gain Stability	Output Impedance	Spurious Outputs
Phase Linearity	AM/PM Conversion	
Phase Stability	Intermodulation Distortion	
Gain Compression	Ambient Temperature Range	
Transmit Freq. Rejection	Overdrive Capability	
Image Freq. Rejection	Shock Requirements	
Size	Vibration/Shock Requirements	

Table I is not complete but it does point out the level of interest that has gone into the parametric amplifier. The paramp noise temperature will now be evaluated with special interest being given to pump AM noise levels.

A. PARAMP NOISE TEMPERATURE ANALYSIS

The noise temperature of a paramp (T_{paramp}) is made up of several separable parts as shown in Figure 3.

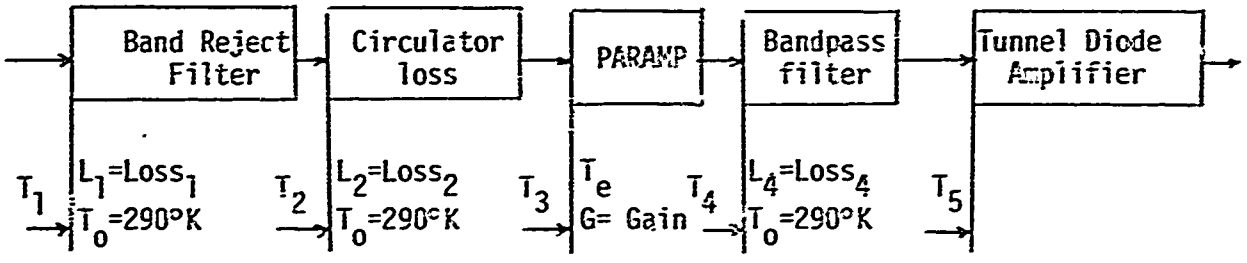

Figure 3. Complete Parametric Amplifier

Where: $T_1 = T_{paramp}$

L_n = Losses for Each Stage

G = Paramp Gain

$$T_{paramp} = (L_1 - 1)T_o - L_1T_2 \quad (11)$$

$$T_2 = (L_2 - 1)T_o - L_2T_3 \quad (12)$$

$$T_3 = T_e + \frac{T_4}{G} \quad (13)$$

$$T_4 = (L_4 - 1)T_o + L_4T_5 \quad (14)$$

T_5 = about 750 Kelvins for a typical Tunnel Diode Amplifier.

Solving for T_{paramp} in terms of the various temperatures and losses:

$$T_{paramp} = (L_1-1)T_o - L_1(L_2-1)T_o + L_1L_2T_e + \frac{L_1L_2(L_4-1)T_o}{G} + \frac{L_1L_2L_4T_5}{G} \quad (15)$$

From Equation 15 it can be observed that the paramp gain should be as large as possible and that the plumbing losses should be made as small as possible.

B. ANALYSIS OF T_e

Figure 4 is an equivalent circuit of a single stage reflex non-degenerate parametric amplifier with a circulator connecting the source to the load. The following assumptions are made: The amplifier has a narrow bandwidth and high gain, the bandwidth of the idler loop is much larger than the signal loop, and the circulator is lossless.

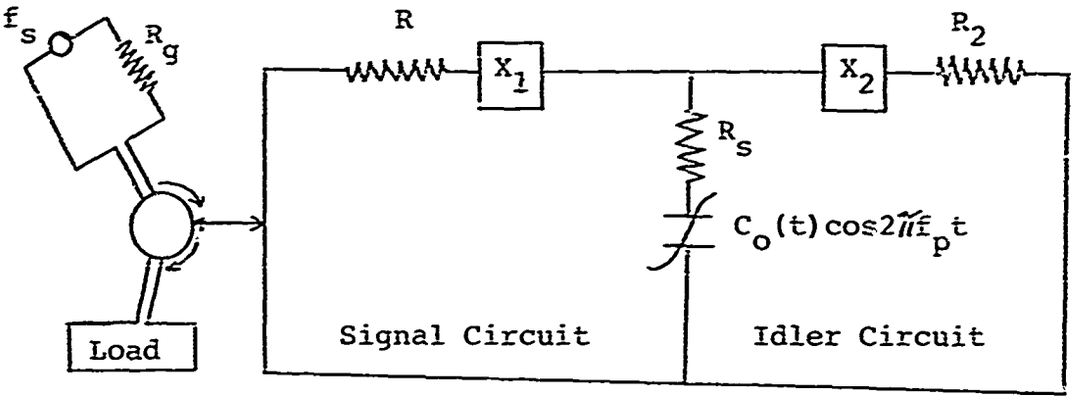

Figure 4. Equivalent Circuit of Nondegenerate Paramp

The Manley and Rowe equations [Ref. 8] are satisfied by the equation:

$$f_{pump} = f_{idler} + f_{signal} \tag{16}$$

Blackwell and Kotzebue in Reference 8 showed that the power gain for the system as described by Figure 4 under matched conditions, is the square of the voltage reflection coefficient. such that:

$$G = \left| \frac{R_g - Z_1}{R_g + Z_1^*} \right|^2 \tag{17}$$

Where: R_g = The circulator impedance

Z_1 = Input impedance of paramp, this will be a negative value since the varactor presents a negative impedance when looking into it

Heffner and Wade [Ref. 6] using an equivalent circuit as shown in Figure 4 considered eight individual noise contributions in deriving the overall noise temperature equation. These eight contributions are:

1. Thermal noise at f_s in the signal circuit.
2. Thermal noise at f_i in the idler circuit.
3. Noise current at f_s emanating from the varactor diode.
4. Noise current at f_i emanating from the varactor diode.
5. Noise fluctuations at f_p in the value of the varactor capacitor.
6. Noise fluctuations at $2f_s$ in the value of the varactor capacitor.
7. Noise fluctuations at $2f_i$ in the value of the varactor capacitor.
8. Noise fluctuations at $(f_s - f_i)$ in the value of the varactor capacitor.

The result of the analysis of the eight individual contributions is Equation 18 modified slightly to give noise temperature instead of noise figure. The definitions of the various terms of the equation are not given here since the equation will only be used to give an insight into the equations that are now used to solve for noise temperature and those portions of the equation that were previously overlooked as being very small or insignificant to other terms of the equation.

Note: G subscript means conductance, G means gain.

Noise fluctuations at $(f_s - f_i)$ are equal and opposite in phase and cancel each other.

$$T_e = T_o \left\{ \overbrace{\frac{G_1}{G_g}}^{1} + \overbrace{\frac{G_2 f_s}{G_g f_i}}^{2} + \frac{1}{4KTBG_g} \left[\overbrace{\overline{i_3}^2}^{3} + \overbrace{\overline{i_4}^2 \frac{G_2 f_s}{G_{T2} f_i}}^{4} \right] \right.$$

$$\left. + \frac{S_i G G_2}{N_i \; 4 \; G_g} \left[\overbrace{\frac{G_2}{G_1} \overline{\rho}^2}^{5} + \overbrace{\frac{G_{T2} f_s}{G_1 f_i} \overline{\sigma}^2}^{6} + \overbrace{\frac{G_2^2 f_s}{G_{T2} G_1 f_i} \overline{\gamma}^2}^{7} \right] \right\} \qquad (18)$$

Where: $\overline{i_3}^2$ = The mean-squared value of the noise current at f_s emanating from the variable capacitance varactor.

$\overline{i_4}^2$ = The mean-squared value of the noise current at f_i emanating from the variable capacitance varactor.

$\overline{\rho}^2$ = The mean-squared value of the ratio of the noise variation at f_p to the coherent variation at f_p in the variable capacitance varactor.

$\overline{\sigma}^2$ = The mean-squared value of the ratio of the noise variation at $2f_s$ to the coherent variation at f_p in the variable capacitance varactor.

$\overline{\gamma}^2$ = The mean-squared value of the ratio of the noise variation at $2f_i$ to the coherent variation at f_p in the variable capacitance varactor.

In the original analysis of Equation 18 all portions of the paramp were assumed to be at the same temperature, in cooled paramps the idler circuit may be cooled to a lower temperature than the signal circuit.

In evaluating the overall noise temperature Heffner and Wade stated that terms 1-2 effectively represented the effective noise temperature arguing that terms 3-4 due to shot noise were very small and that terms 5-7 were probably unimportant in any physical embodiment. Thus based on all the

approximations used the effective noise temperature could be written as:

$$T_e = T_o \left[\frac{G_1}{G_g} + \frac{G_2 f_s}{G_g f_i}\right] \tag{19}$$

This equation, or various other forms of it, may be found in much of the modern literature concerning paramp noise temperature. When it was recently discovered that the paramp noise temperature increased significantly when a large interfering signal was in or near the paramp passband, especially when solid state pumps were used, many designers were puzzled and hard pressed to explain why. A re-examination of Equation 18 will give an immediate clue to what caused the increased noise temperature. Rewriting terms 5-7:

$$\frac{S_i G G_2}{N_i\ 4\ G_g} \left[\underset{5}{\frac{G_2}{G_1}\ \bar{\rho}^2} + \underset{6}{\frac{G_{T2} f_s}{G_1 f_i}\ \bar{\sigma}^2} + \underset{7}{\frac{G_2{}^2 f_s}{G_{T2} G_1 f_1}\ \bar{\gamma}^2}\right] \tag{20}$$

It may readily be seen that if S_i is a large interfering signal then terms 5-7 must be reconsidered. Each of these terms will now be considered on a separate basis to see if any approximations can be made. For modern paramps f_i, the idler frequency, is much much greater than f_s, the signal frequency, by a factor of between five to nine. $\bar{\sigma}^2$ is the mean squared ratio of the noise variation at $2f_s$ to the coherent variation at f_p in the varactor and $\bar{\gamma}^2$ is the mean squared value of the ratio of the noise variation at $2f_i$ to the coherent variation at f_p in the varactor. Since both frequencies are not in or

near the bandwidth of the idler circuit and also both of these terms have the ratio f_s/f_i, terms 6 and 7 have very small contributions and may be neglected, when compared to the contribution made by term 5. Term 5 does not contain the signal to idler frequency ratio and the term $\overline{\rho}^2$ is the mean squared value of the ratio of the noise at f_p to the coherent variation at f_p. The AM noise of an oscillator can cause power fluctuations and is sometimes referred to as coherent noise. The AM noise level of a klystron is much smaller than the AM noise level of some solid state oscillators, therefore, $\overline{\rho}^2$ must be considered. Rewriting Equation 18 using these arguments:

$$T_e = T_o \left[\frac{G_1}{G_g} + \frac{G_2 f_s}{G_g f_i} + \frac{S_i G G_2^2}{N_i \ 4 G_g G_1} \ \overline{\rho}^2 \right] \qquad (21)$$

This equation accounts for the increase in noise temperature when a high level interfering signal (S_i) is in or near the paramp passband.

Since $\overline{\rho}^2$ may be attributed to the AM pump noise level it explains why, for a given interfering signal level the paramp noise temperature will vary from pump source to pump source.

Although Heffner and Wade's equation gives the paramp designer an insight into the individual noise contributions to the overall noise temperature, it is very difficult to evaluate or measure the individual conductances. Equation 21 may be looked at as two separate parts; the first two noise terms when no interfering signal is present, and the last term when the interfering signal is large and the overall contribution

caused by this signal over-shadows all other contributions. Equation 21 may be re-written as:

$$T_e = T_{e1} + T_{e2} \tag{22}$$

Where:

$$T_{e1} = T_o \left[\frac{G_1}{G_g} + \frac{G_2 f_s}{G_g f_i} \right] \tag{23}$$

$$T_{e2} = T_o \left[\frac{S_i G G_2^2}{N_i \ 4 G_g G_1} \ \bar{\rho}^2 \right] \tag{24}$$

T_e will now be evaluated separately so that a system user will be able to calculate the approximate noise temperature that he may anticipate when pumping with any type of source with or without an interfering signal.

To illustrate the effect of a high level interfering signal in conjunction with a noisy pump upon the paramp noise temperature Figures 5-8 can be compared. For all of the measurements the following values were equal: Pump power, pump frequency, paramp gain.

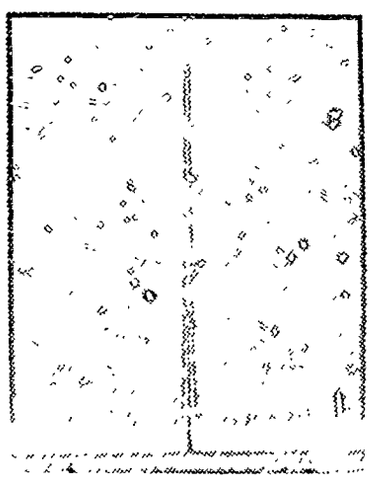

Figure 5. Silicon Impatt pump frequency spectrum

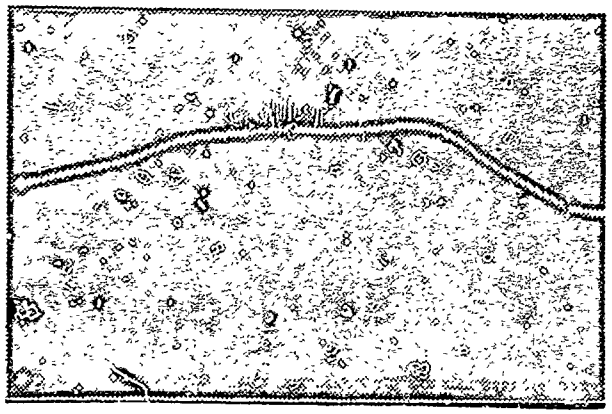

Figure 6. Paramp Passband, markers result from wavemeters, paramp gain is 10 db

The silicon impatt frequency spectrum in Figure 5 can be considered as a good spectrum when compared to Figure 7 and was the best spectrum obtained with this particular device. Noise temperature measurements were made with and without an interfering signal.

With $S_i = 0$ $T_{paramp} = 175$ Kelvins

$S_i = -50$ dbm $T_{paramp} = 297$ Kelvins

Figure 7. Silicon Impatt Pump Frequency Spectrum, (Detuned)

Figure 8.

Paramp Passband

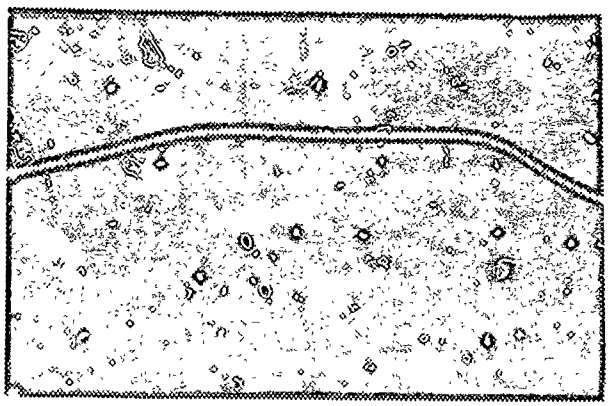

Note: Even with the very poor pump spectrum the paramp gain could still be achieved. There is no indication of the poor pump spectrum in the paramp passband.

The silicon impatt frequency spectrum as photographed in Figure 7 is not typical, but was detuned especially to show that pump noise can have a very degrading effect on the paramp noise temperature.

With: $S_i = 0$ $T_{paramp} = 297$ Kelvins

$S_i = -50$dbm $T_{paramp} = 1490$ Kelvins

Comparing the two pump spectra, and realizing that the spectrum of Figure 7 is not typical, in the absence of an interfering signal the paramp temperature has changed very little. However when the signal is present the change is very significant.

C. T_{el} (PARAMP NOISE TEMPERATURE IN THE ABSENCE OF AN INTERFERING SIGNAL)

Penfield and Rafuse [Ref. 7] derived several equations using a paramp noise temperature analysis very similar to that of Heffner and Wade [Ref. 6]. These equations may be found in nearly all of the present day literature on paramps. A few of the more important equations are:

$$T_{el} = T_o \frac{f_s}{f_i} \left[\frac{(mf_c)^2 + f_i^2}{(mf_c)^2 - f_s f_i} \right] \quad (25)$$

$$f_{popt} = \sqrt{mf_c^2 + f_s^2} \quad (26)$$

$$P_{pump} = CP_{norm} \left(\frac{f_p}{f_c} \right)^2 \quad (27)$$

$$\frac{\Delta G}{G} = \frac{G-1}{\sqrt{G}} \frac{\Delta P_p}{P_p} \quad (28)$$

Where: T_o = 290 Kelvins assumed although it should actually be the operating temperature of the paramp.

m = Varactor diode factor that varies with material and is approximately .25 for G_aA_s varactor.

f_c = Varactor diode cutoff frequency.

f_{popt} = Optimum pump frequency resulting in minimum noise temperature.

P_p = Relative pump power required to pump the varactor diode to give desired paramp gain.

C = Derived constant for a given diode.

P_{norm} = Normalized pump power.

$\frac{\Delta G}{G}$ = Paramp gain sensitivity.

$\frac{\Delta P}{P}$ = Pump power variations normalized.

In looking at Equation 75 two facts become immediately apparent that will reduce the value of T_{el}. If the pump frequency could be increased the idler frequency would also be increased while

the signal frequency remains fixed in value since $f_p = f_s + f_i$. The second fact is that if the Varactor cutoff frequency (f_c) could be increased T_{el} could also be reduced. In fact if the cutoff frequency could be increased to an extremely high value the noise temperature becomes a ratio of the signal frequency to the idler frequency. As an example using typical values of present day paramps:

$f_c = 280$ GHz
$m = .25$
$P_p = 200$ mw
$f_p = 42$ GHz
$f_s = 7.5$ GHz

$$T_{el} = 290 \left[\frac{7.5}{34.5}\right] \left[\frac{70^2 + 34.5^2}{70^2 - 34.5*7.5}\right]$$

$$T_{el} = 82\ ^\circ K$$

From Equation 26 there is an optimum pumping frequency;

$$f_{popt} = \sqrt{70^2 + 7.5^2}$$

$$= 70\ 4 \text{ GHz}$$

If the paramp were pumped at this frequency a new noise temperature of 69 °K would result, however, look at the penalty that must be paid in the additional required pump power. From Equation 27:

$$P_{pump} = CP_{norm} \left[\frac{f_p}{f_c}\right]^2 \quad \text{if } P_{pump} = 1 \text{ for the 42 GHz pump}$$

Three times the pump power would be required to pump at 70 GHz, not very practical with solid state sources.

Since it is not practical to pump at 70 GHz due to the required pump power it may be more practical to use a varactor with a cutoff frequency of about 500 GHz. With a varactor of this

cutoff frequency a paramp noise temperature of 69 °K would again result. More important is the fact that the required pump power would be one third as much, still referencing the 42 GHz pump.

In recent solid state technological advances two things have happened that has put even more emphasis on the use of a parametric amplifier. These developments include a new high power solid state pump and a higher cutoff frequency varactor diode. Dickens [Ref. 9] reported that an uncooled X-Band parametric amplifier using a varactor diode with a zero bias cutoff frequency of 600 GHz and pumped at 70 GHz had been developed that had an excess noise temperature of 63 °K.

D. ANALYSIS OF T_{e2} (NOISE TEMPERATURE CONTRIBUTION CAUSED BY THE PRESENCE OF AN INTERFERING SIGNAL)

The paramp noise temperature in the presence of an interfering signal was found to be a function of T_{e2}. Where:

$$T_{e2} = T_o \frac{S_i G G_2^2}{N_i \; 4 G_g G_1} \; \overline{\rho}^2 \quad ; \text{ G subscripts are conductances}$$

Also:

$$\frac{\Delta G}{G} = \frac{G - 1}{\sqrt{G}} \quad \frac{\Delta P_p}{P_p} \quad ; \text{ G = Gain}$$

In looking over these equations very closely, both equations have gain terms and also a term that is pump function. A thorough analysis of the paramp gain sensitivity equation will lead to a solution that can be used to calculate T_{e2} directly.

Figure 9 is an amplifier that shows some common, well known relationships.

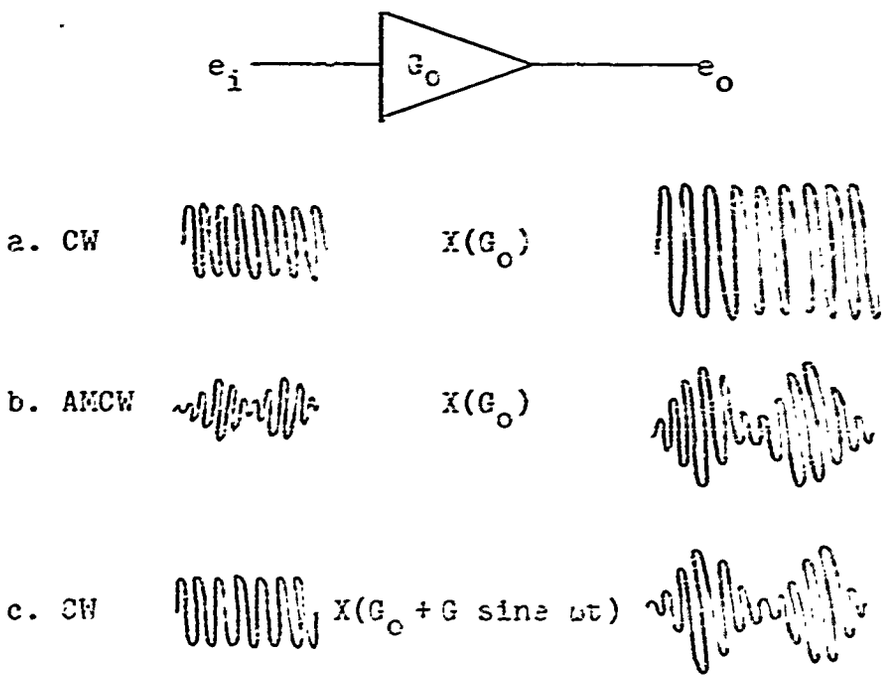

Figure 9. Amplifier With Gain G_o

Note that the amplifier with a periodic gain variation has an output that appears the same as the amplifier with an AMCW input. For very short periods of time ΔG in the gain sensitivity equation, Equation 28, may appear to be periodic. Assuming that it is periodic for very short durations of time we can say that it is the same as having an AMCW input into an amplifier of Gain G_o. Figures 10 and 11 show the power and phasor relationships of double-sideband amplitude modulated signal.

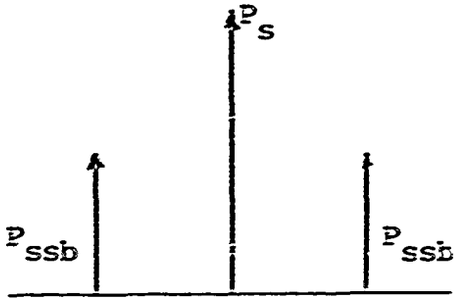

Figure 10. AMCW Signal Spectrum (sb indicates sidebands)

P_s = carrier power

P_{ssb} = power in each sideband

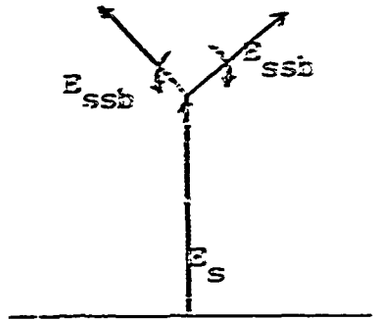

Figure 11. Phasor Diagram of an AMCW Signal

E_s = carrier voltage

E_{ssb} = sidebands

In Figures 10 and 11 no frequency has been assigned since we are allowing the interfering signal P_s to be in or near the passband and since we assumed that ΔG was periodic over a very short period of time, the sideband frequencies will in actuality be random about the carrier frequency. What is needed, is to know the amount of sideband power that can cause the same result in the output as a small change in gain over a short period of time. From the phasor diagram:

$$E_{max} = E_s + 2E_{ssb} \tag{29}$$

$$P_s = E_s^2 \tag{30}$$

$$P_{smax} = (E_s + 2E_{ssb})^2 \tag{31}$$

$$P_{smax} = E_s^2 + 4E_sE_{ssb} + 4E_{ssb}^2 \tag{32}$$

$$\Delta P_s = P_s - P_{smax} = 4E_sE_{ssb} + 4E_{ssb}^2 \tag{33}$$

In this case (and in reality) the paramp gain variations are very small, therefore, E_{ssb} is very much smaller than E_s. Equation 33 may then be rewritten:

$$P_s = 4E_sE_{ssb} \tag{34}$$

Normalizing;

$$\frac{\Delta P_s}{P_s} = \frac{4E_sE_{ssb}}{E_s^2} \tag{35}$$

Since $P_s = E_s^2$ and $P_{ssb} = E_{ssb}^2$ then:

$$\frac{\Delta P_s}{P_s} = 4\sqrt{\frac{P_{ssb}}{P_s}} \tag{36}$$

From this equation and knowing that a change in parametric amplifier gain caused the same output as an amplitude modulated input signal into an amplifier with constant gain. Then from the gain sensitivity equation:

$$4\sqrt{\frac{P_{ssb}}{P_s}} = \frac{\Delta G}{G} = \frac{G-1}{\sqrt{G}}\,\frac{\Delta P_p}{P_p} \tag{37}$$

Since ΔG is a totally random process over a long period of time, only being viewed as periodic for very short periods, then P_{ssb} may also be viewed as an Input Noise Power level. It will be shown that ΔP_p is totally random and that P_{ssb} can be viewed in this manner. In order to evaluate the term $\Delta P_p/P_p$ (normalized pump power variations), the power spectrum of a typical oscillator will be examined. Figure 12 shows an oscillator of frequency f_p, power P_p with a symmetrical AM noise distribution about it.

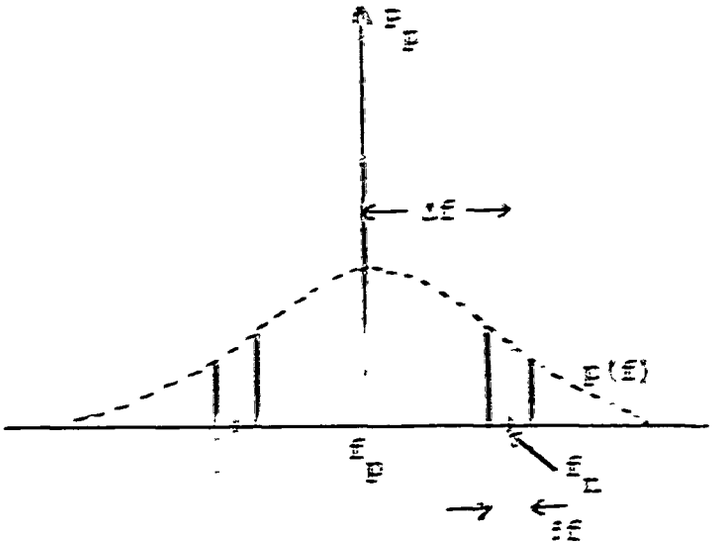

Figure 12. Oscillator Power Spectrum with AM Noise

From Figure 12 $f_n = f_p + \Delta f$ and p(f) is the AM noise power distribution function. The total amount of noise power centered about f_n is:

$$P_{pssn} = p(f)\Delta f = \int_{f_n-\Delta f/2}^{f_n+\Delta f/2} p(f)\, df \qquad (38)$$

Where: P_{pssn} is the single-sideband noise power located about Δf and centered about f_n.

If Δf was very small and the entire noise spectrum was divided into small segments then the various amounts of power contained in each segment could be calculated using Equation 38. If this were done then the noise power in each segment could be thought of as a delta function containing a quantized noise power of P_{pssn}. Figure 13 then portrays Figure 12 only with the noise quantized.

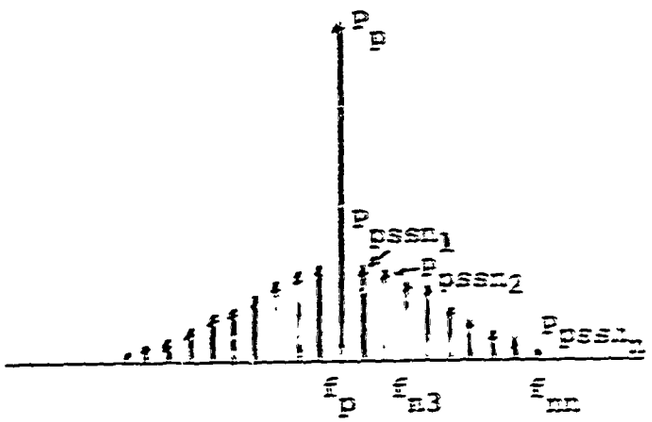

Figure 13. Oscillator Power Spectrum with Quantized AM Noise

The AM noise level of an oscillator is well known to be totally random in nature. At any instant of time any one of, but not all of the quantized noise Delta functions may be present. If one were to add all of the noise powers and divide by (n) you would have an average level of the AM sideband noise level. Thus for a very short period of time the AM noise having power P_{pssn} may be centered about $f_p + f_{n3}$ and $f_p - f_{n3}$ as shown in Figure 14.

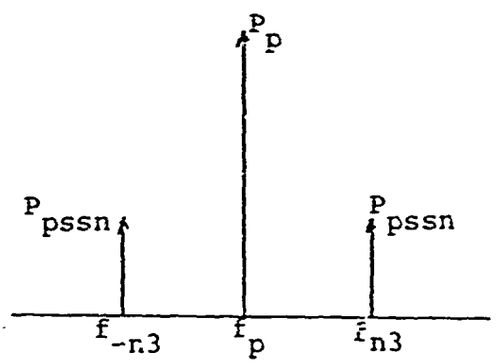

Figure 14. Oscillator Power Spectrum (Instantaneous)

Figure 14 now appears similar to an AM double side-band signal. This view will change very rapidly, however, if one could take photographs from instant to instant the resulting photograph may appear very similar to Figure 14. Accepting this view as one of the many ways that AM noise may be visualized, realizing that there are as many ways of describing AM noise as there are authors. Then using the same analysis as was used in evaluating Figure 10 we find that:

$$\frac{P_p}{P_p} = 4\sqrt{\frac{P_{pssn}}{P_p}} \tag{39}$$

substituting into equation (37):

$$4\sqrt{\frac{P_{ssb}}{P_s}} = \frac{G - 1}{\sqrt{G}} \; 4\sqrt{\frac{P_{pssn}}{P_p}} \tag{40}$$

Squaring both sides of the equation:

$$\frac{P_{ssb}}{P_s} = \frac{(G - 1)^2}{G} \; \frac{P_{pssn}}{P_p} \tag{41}$$

Thus the final result does show that the term P_{ssb} is totally random and may be considered as the sideband noise power of the input signal. If G>10, Equation 41 can be rewritten as:

$$P_{ssb} = P_s \; G \; \frac{P_{pssn}}{P_p} \tag{42}$$

P_{ssb} is the noise power that shows up in the input of a paramp as a result of a power fluctuation in the paramp pump. It has

been shown that this pump power fluctuation was the result of the AM noise in the pump itself and as was mentioned earlier this AM noise power varies depending upon the type of source being used. The entire derivation of Equation 42 was done considering a very narrow noise bandwidth and in fact is noise power per hertz bandwidth. Since P_{ssb} is noise power spectral density:

$$P_{ssb} = KT = \text{noise power per Hz bandwidth} \quad (43)$$

Where: K is Boltzman's constant

T is the equivalent noise temperature and is the T_{e2} that is desired.

$$P_{ssb} = KT_{e2} = P_s\, G\, \frac{P_{pssn}}{P_p} \quad (44)$$

solving for T_{e2}:

$$T_{e2} = P_s\, G\, \frac{P_{pssn}}{K P_p} \quad (45)$$

Where: T_{e2} is the contribution to the paramp input noise temperature which is linearly proportional to the interfering signal power, paramp gain, and pump AM noise level

This result accounts for the increase in noise temperature when an interfering signal is in or near the paramp passband, is a function of the paramp gain, and pump AM noise power. All the major terms of Heffner and Wade's equation are accounted for and it is the solution being sought. This result is in agreement with the work done by Chramiec [Ref. 10-11] who published his result in the form of a paramp output signal to

noise ratio degradation. His derivation was based upon auto-correlation techniques and was not at all similar to the approach used herein. Recall that $T_e = T_{e1} + T_{e2}$ thus the overall equation can be written as:

$$T_e = T_o \frac{f_s}{f_i} \left[\frac{(mf_c)^2 + f_i^2}{(mf_c)^2 - f_s f_i} \right] + P_s G \frac{P_{pssn}}{KP_p} \qquad (46)$$

This equation must be substituted into the overall equation that accounts for all of the paramp losses in order to solve for T_{paramp}. Since the various loss values and pump frequencies may vary from paramp to paramp the overall equation for T_{paramp} will not be investigated. What is important is that T_{paramp} is equal to a constant times T_e. A good understanding of the above equation can, for a given paramp having a gain G, and a pump whose approximate AM noise level is known, a known level of interfering signal power, predict the input noise temperature.

As an example of the kind of information that can be obtained let:

$$T_e = 100\ ^\circ K + P_s G \frac{P_{pssn}}{KP_p} \qquad (47)$$

Where: 100 Kelvins is the noise temperature with no interfering signal

P_{pssn}/P_p is the AM noise level for various pumps

G = Paramp Gain

K = Boltzman's constant

T_e can be plotted for various values of interfering signal power and various levels of AM pump noise. Figure 15 is such a plot.

From Figure 15 note that a paramp having a pump with a low AM noise level can have very high interfering signal powers before the paramp noise temperature is degraded. It has been reported by Wagner and Gray [Ref. 12] that an unstabilized silicon impatt pump may have an AM noise level on the order of -100 db/KHz. Klystrons have AM noise levels on the order of -130 db/KHz. (This is a very significant difference if paramp operation in the presence of an interfering signal must be considered.)

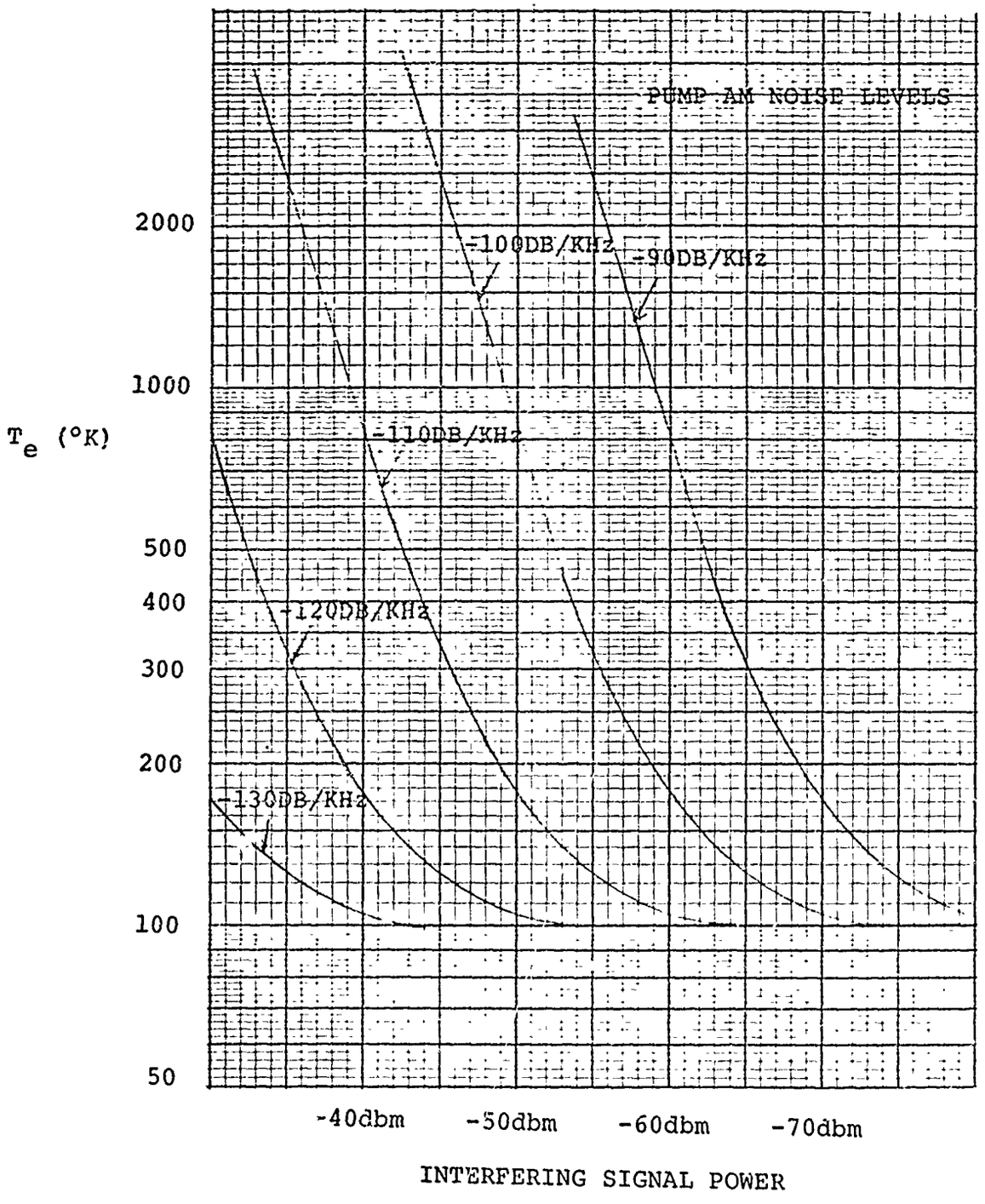

Figure 15. T_e Versus Interfering Signal Power for Various Levels of AM Pump Noise

III. NOISE TEMPERATURE MEASUREMENTS

The laboratory experiments were made on an AIL model 2942 low noise parametric amplifier stage built by AIL for use in the AN/MSC-57 SHF tactical satellite terminal. This amplifier was entirely self contained, easily tuned, and the pump mount allowed for easy adaptation of the various sources to be investigated.

Table II. AIL Model 2942 Paramp Parameters

operating frequency	7.25 - 7.75 GHz tuneable
bandwidth	60 MHz minimum
noise temperature	less than 190°K, typical 140°K
gain	18 db
pump (Varian 302) Klystron	41.8 GHz ± 1%, 200 mwatts typical, 150 mwatts minimum required to achieve an 18 db gain

Figure 16 is a display of three solid state pumps, a Varian 302 Klystron, and the Alpha (Sylvania) tripler that were used to investigate noise temperature.

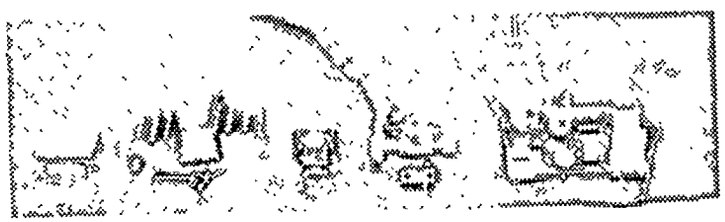

Figure 16. Left to Right: Hughes 44019, Monsanto Vu 2626A, Varactor Tripler, Varian VA 302, Alpha (Sylvania) SYG-2036-99.

All of the sources are shown without power supplies and matching devices that were used for the tests.

Table III. Significant Parameters of Various Pump Sources

Source	Manufacturer	Type	Freq.	Bias Voltage	Bias Current	Power Output
44019	Hughes	Silicon Impatt	42GHz	29 V	.2 A	200 mw @ 42GHz
VU-2626A	Monsanto	Gunn	14GHz	7.6 V	3.6 A	400 mw @ 14GHz
VA-302	Varian	Klystron (reflex)	42GHz	Beam 900V Ref. 1350V	.03A	200mw @ 42GHz
SYG-2036-99	Alpha (Sylvania)	Silicon Impatt	14GHz	115 V	.08A	200mw @ 14GHz

The varactor tripler was supplied with the Alpha Silicon Impatt pump.

In order to measure the input noise temperature of the paramp a set-up similar to Figure 17 was used

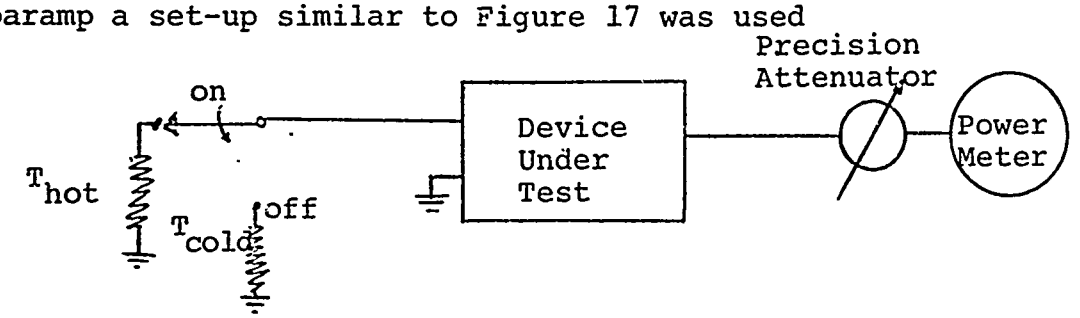

Figure 17. Simple Noise Temperature Test Set-Up

The two thermal noise sources each produce noise power proportional to their given temperatures. The output power can be measured for each noise source temperature. Defining:

$$Y = \frac{P_{hot}}{P_{cold}} \tag{48}$$

Where: P_{hot} = resulting power from the hot source.

P_{cold} = resulting power from the cold source.

The input noise temperature is then given by:

$$T_e = \frac{T_{hot} - YT_{cold}}{Y - 1} \qquad (49)$$

The addition of the precision attenuator allows the two output powers to be compared directly without actually reading the absolute power of each source. This is called the Y-Factor method for noise temperature measurement.

In order to make actual paramp input noise temperature measurements the AIL Type 136 precision test receiver, and Type 70 noise discharge gas tube were used. The precision test receiver allows for a direct reading of the Y-Factor from a precision attenuator dial.

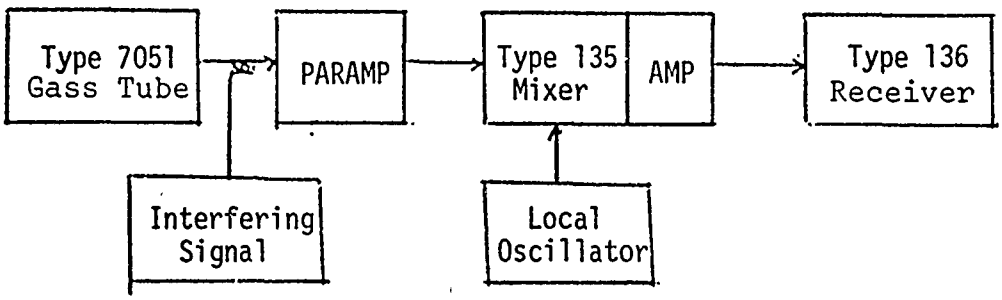

Figure 18. Test Set Up for Noise Temperature Measurement Using AIL Equipment.

The total noise power delivered by the paramp is proportional to the paramp's bandwidth by the equation:

$$P_{\text{noise power}} = KTB \qquad (50)$$

with the addition of the local oscillator and mixer the noise power over a small portion of the overall paramp passband can be measured.

Figure 19 illustrates the relationship between the local oscillator, mixer, and interfering signal frequencies.

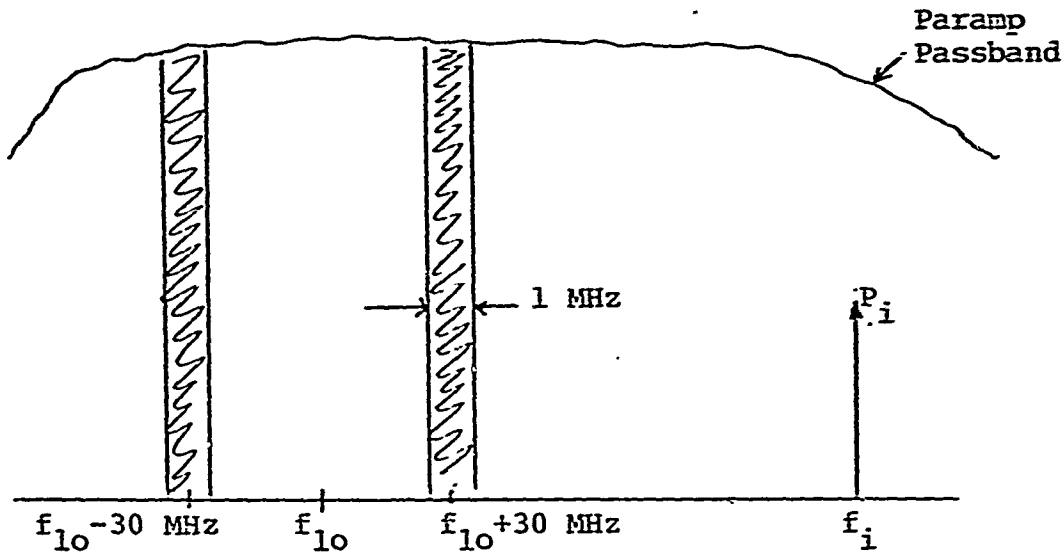

Figure 19. Local Oscillator, Mixer, Interfering Signal Frequency Relationship.

With the local oscillator and mixer it is possible to make noise temperature measurements anywhere within the paramp passband thus for actual measurements the local oscillator was set at the low end and the interfering signal was set at the high end of the paramp passband. The amplifier following the mixer amplifies the noise power before it is attenuated and read on the Type 136 power meter. The Type 135 Mixer and amplifier adds to the overall noise temperature of the system. By connecting the gas noise generator directly to the input of the mixer the second stage temperature contribution could be measured and from:

$$T_{es} = T_{paramp} + \frac{T_{mixer}}{\text{Gain Paramp}} \qquad (51)$$

The second stage noise temperature may be subtracted from the overall system noise temperature to give the paramp noise temperature:

$$T_{paramp} = T_{es} - \frac{T_{mixer}}{\text{Gain Paramp}} \tag{52}$$

From Figure 17 and Equation 49 the value of T_{hot} and T_{cold} must be known in order to solve for the system temperature based on the value of the Y factor measured. The excess noise ratio for the AIL type 7051 noise generator is 15.75 db. The paramp input loss due to couplers, circulator, and a band reject filter was estimated to be about 1/2 db. Thus the approximate values of T_{hot} and T_{cold} could be calculated.

$$T_{ex} = \frac{(T_{hot} - 290)}{290} \tag{53}$$

$$T_{hot} = 290(1 + T_{ex}) \tag{54}$$

$$T_{hot} = 10{,}000\ ^{\circ}K$$

$$T_{cold} = 290\ ^{\circ}K \quad \text{(assumed)}$$

The mixer-amplifier (2nd stage) temperature was measured to be 1000 Kelvins

$$T_{paramp} = \frac{10{,}000 - Y290}{Y - 1} - \frac{1000}{\text{Gain Paramp}}\ ^{\circ}K \tag{55}$$

NOTE; This equation is approximate, since the input loss and T_{cold} were estimated, what is important is that since the same values were used for all measurements, the various temperatures measured when using different pumps can be compared.

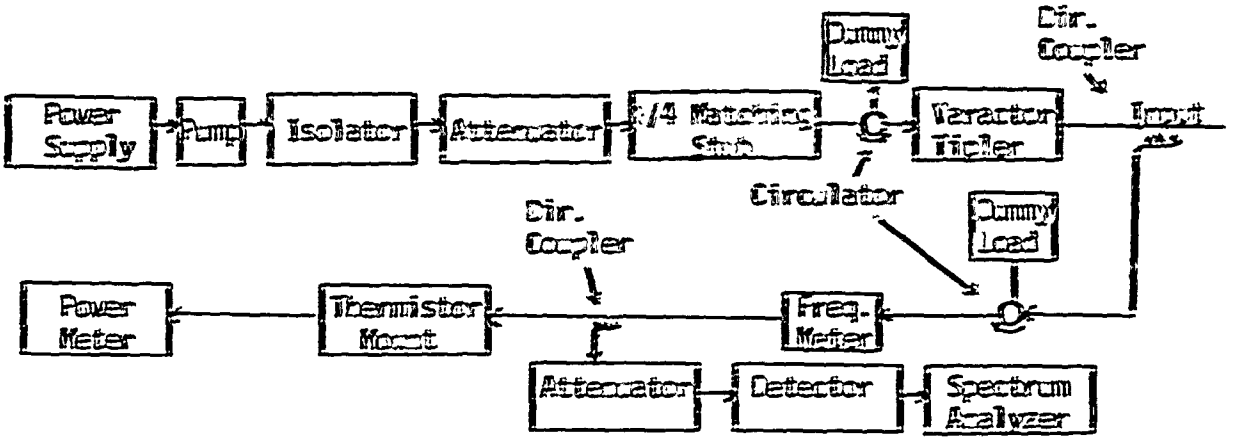

Figure 20. Pump Power, Frequency, and Spectrum Monitering System.

In order to observe the paramp gain a sweep generator was connected at the paramp output. Figure 21 is a photograph of the paramp passband resulting from a sweep generator input.

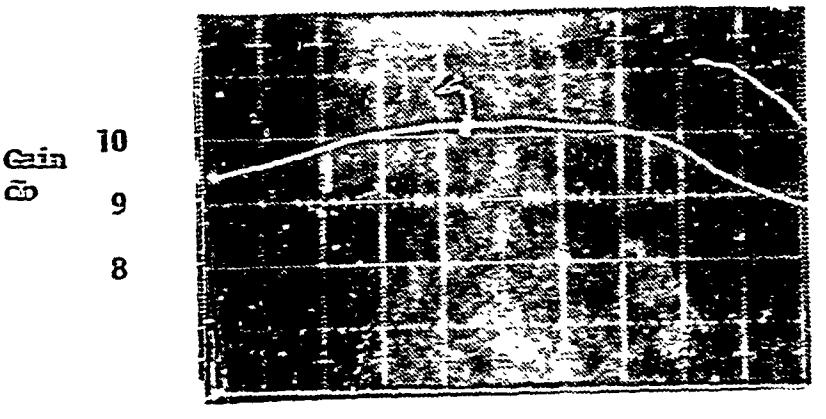

Figure 21. Paramp Passband Resulting From Sweep Generator Input, Notches are used for Tuning Only.

Figure 22 is a diagram of the complete laboratory set-up. Using this set-up, the interfering signal power was carefully measured and with the use of a well calibrated attenuator in the signal circuit the input power into the paramp could be carefully controlled. With each of the separate pumps the same procedure was used. Each pump delivered the same amount of power at the same frequency to the paramp. The paramp gain and passband were adjusted by slight variations of the varactor diode bias adjustment. Figure 23 is a plot of one set of data taken, which can be compared to the theoretical curves of Figure 15. The second stage temperature contribution has been subtracted for this plot. No data could be taken for an interfering signal power greater than -40dbm due to mixer limitations. It would not be expected that any interfering signal would exceed -60dbm under any operating conditions. The reference lines were plotted for the equation:

$$T_{paramp} = 140\ ^{\circ}K \div P_s \frac{P_{pssn}}{KP_p}\ ^{\circ}K \qquad (56)$$

where: P_s = Interfering signal power

G = Paramp gain, 8.5db

P_{pssn}/P_p = AM noise levels

Figure 23 is one of many plots that were made and was considered typical by the author. The difference in frequency between the local oscillator and interfering was varied for some of the data not shown here. The Alpha Impatt pump was very difficult to tune due to the fact that maximum power was

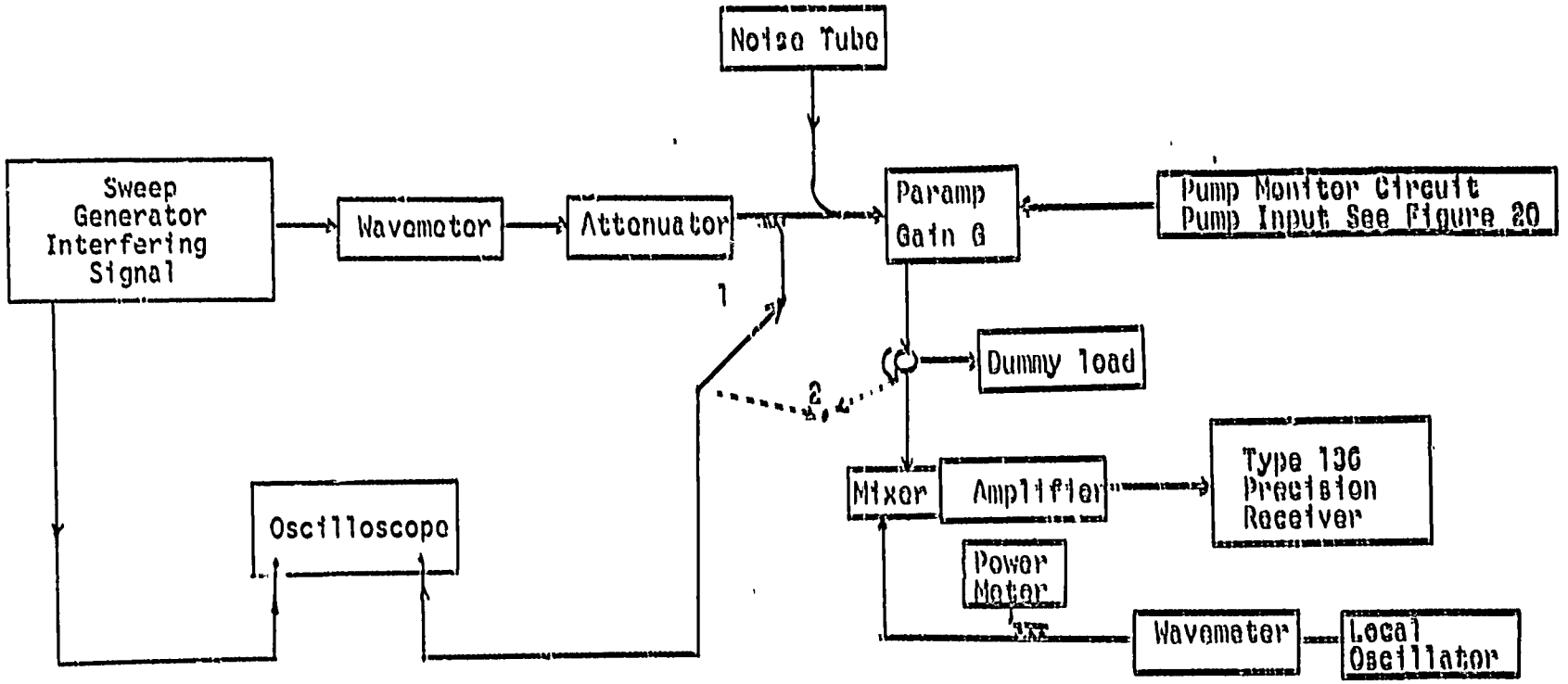

Figure 22. Complete Laboratory Set-Up for Measuring Paramp Input Noise Temperature In the Presence of an Interfering Signal.

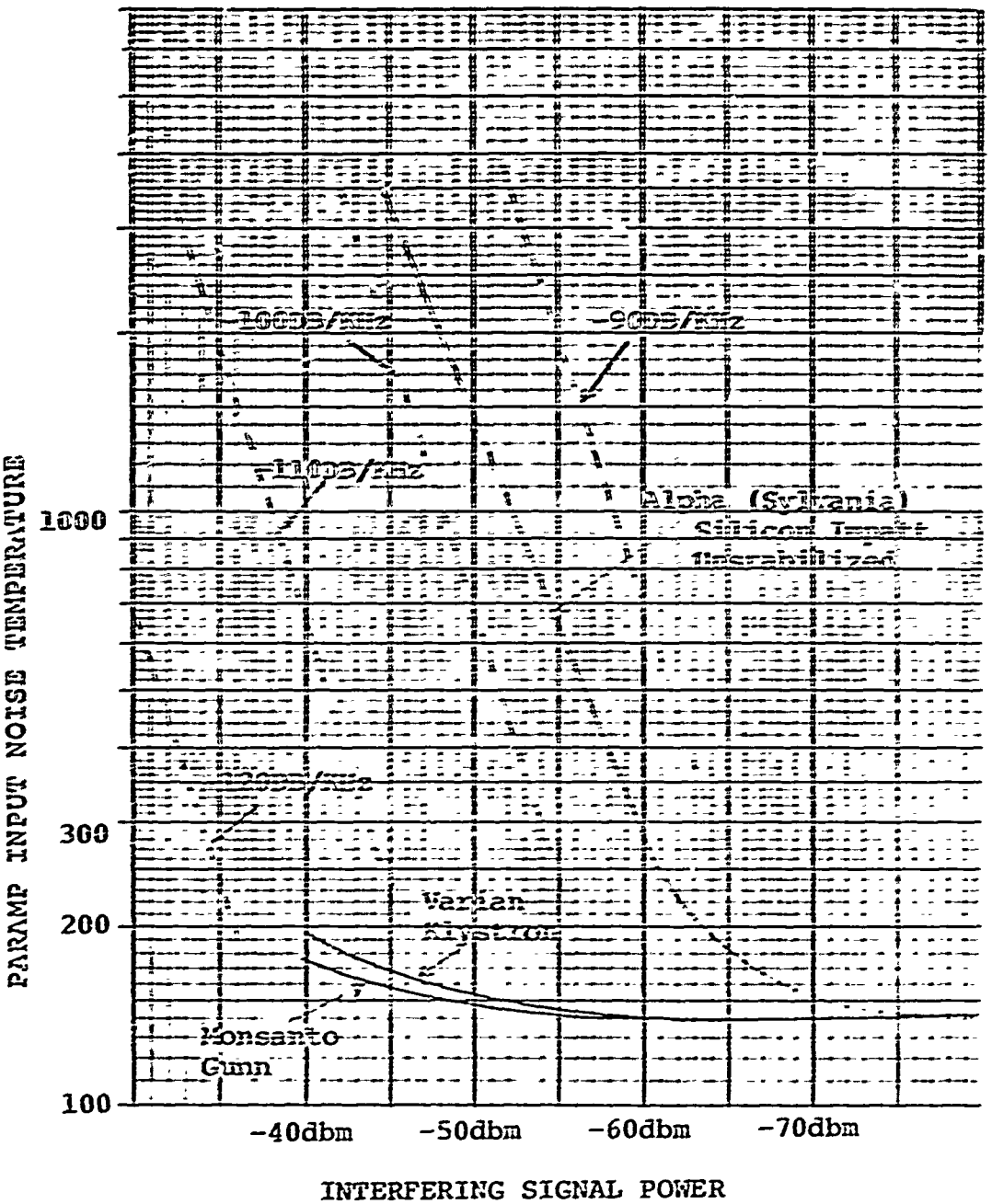

Figure 23. Paramp Input Noise Temperature Versus Interfering Signal Power.

Note: Data with Monsanto Gunn gave the AM noise level as being -123 db bandwidth unspecified, but believed to be KHz.

desired. Depending on how well the impatt was tuned, the data points would fall between the (-90 to -110) AM noise lines, but in any case the resulting plot would appear as the plot shown. This wide variation can be attributed to early design problems in pump construction. With the more modern design techniques now being used this wide variation should be eliminated. The Hughes silicon impatt was not plotted since the data was incomplete, a power supply casualty caused the impatt to fail. Since for this experiment the pump AM noise levels were not known to any degree of accuracy, and were not measured, based on past history of reported AM noise levels, the results tentatively verify the equation derived to predict paramp input noise temperature.

The results of Figure 23 parallel the results obtained by Regan [Ref. 3], when he was working with 35 GHz pumps. Regan is continuing work in this area at NELC San Diego, and with higher power pumps will be able to increase the data base and may be able to place specifications on the maximum allowable AM noise level permitted for military paramp applications.

IV. CONCLUSIONS

In conclusion, a new equation has been derived that will predict the paramp input noise temperature for various pump AM noise levels under interfering signal conditions. The final equation with an accompanying plot shows that if no interfering signal is in or near the paramp passband then the paramp input noise temperature is independent of the pump AM noise level. However, measurements show that high AM noise levels will in fact cause a slight increase in temperature. The plot also shows that if one of the considerations of paramp operation is the possible presence of an interfering signal in or near the paramp passband, then the pump with the lowest noise level should be used. Experimental measurements were in agreement with the derived equation. In any case, for lowest input paramp noise temperature operation the paramp should be constructed with the highest quality varactor diode that is pumped at the highest practical frequency and the pump with the lowest available AM noise level should be used.

BIBLIOGRAPHY

1. Naval Electronics Laboratory Center Technical Note 1592, Principles of Parametric Amplification, by K. D. Regan, 5 December 1969, Tentative and Unpublished.

2. Naval Electronics Laboratory Center Technical Note 1840, Recommended Solution to Certain Problems Associated with the Navy Satcom Paramp Development, by K. D. Regan, 21 April 1971, Tentative and Unpublished.

3. Naval Electronics Laboratory Center Technical Note 1923, Parametric Amplifier Pump Source Investigation Semi-Annual Progress Report, by K. D. Regan, 30 August 1971, Tentative and Unpublished.

4. Naval Electronics Laboratory Center Technical Note The Application of Parametric Amplifiers in SHF Satcom Systems, by K. D. Regan, 8 February 1972, Tentative and Unpublished.

5. Philco (Ford) Technical Memo 162, Ultralow-Noise Parametric Amplifiers in Communication Satellite Earth Terminals, by C. Cuccia, p. 1-13-16, November 1969.

6. Heffner, H. and Wade, G., "Gain, Bandwidth, and Noise Characteristics of the Variable Parameter Amplifier," Journal of Applied Physics, Vol. 29, no. 9, p. 1321-1331, September, 1958.

7. Penfield, P. and Rafuse, R., Varactor Applications, M.I.T. Press, 1962.

8. Manley, J. and Rowe, H., "Some General Porperties of Nonlinear Elements-Part I. General Energy Relations," Proceedings of IRE, p. 904-913, July 1956.

9. Dickens, L., "A Millimeter-Wave Pumped X-Band Uncooled Parametric Amplifier," Proceedings of IEEE, p. 328-329, March 1972.

10. Chramiec, J., "Effect of Pump Noise and Interfering Signal in Parametric Amplifiers," Proceedings of IEEE, p. 149, January 1972.

11. Chramiec, J., "Analysis of the Effect of Pumping Generator Noise on the Specific Properties of a Parametric Amplifier," Gdansk Polytechnic Institute, Archiwun Elecktrotechniki, Vol. 20, No. 1, 1971.

12. Hughes Aircraft Company Technical Report P72-68, 42-GHz Solid State Parametric Amplifier Pump, by Wagner R. and Gray W., p. 51, March 1972.